

Methylation of $[\text{Pt}_2(\mu\text{-SR})(\mu\text{-S})(\text{PPh}_3)_4]$: En Route to Mixed-Thiolato Bridged Complexes

Siew Huay Chong,^[a] Lip Lin Koh,^[a] William Henderson,^[b] and T. S. Andy Hor*^[a]

Abstract: Sequential and independent alkylation of $[\text{Pt}_2(\mu\text{-S})(\text{PPh}_3)_4]$ by RX followed by methylation with Me_2SO_4 led to the first successful isolation of novel diplatinum complexes $[\text{Pt}_2(\mu\text{-SR})(\mu\text{-S-CH}_3)(\text{PPh}_3)_4](\text{PF}_6)_2$ (**3**) (R = $\text{CH}_2\text{C}_6\text{H}_5$ (**a**), CH_2CHCH_2 (**b**), $\text{C}_5\text{H}_{10}\text{CO}_2\text{CH}_2\text{CH}_3$ (**c**), $\text{C}_2\text{H}_4\text{CO}_2\text{-CH}_2\text{CH}_3$ (**d**), $\text{CH}_2\text{CH}_2\text{CN}$ (**e**), $\text{C}_2\text{H}_4\text{CH}(\text{O})_2\text{C}_2\text{H}_4$ (**f**), and $\text{C}_2\text{H}_4\text{SC}_6\text{H}_5$ (**g**)) with asymmetric thiolato bridges. The synthetic methodology can tolerate a range of electronically and sterically contrasting thiolate substituents with

different chemical functionalities. The X-ray crystal structures of **3a-c, g** confirm the unusual heterodialkylation with two different thiolato bridging ligands in a *syn-exo* conformation. A secondary product $[\text{Pt}_2(\mu\text{-SC}_2\text{H}_4\text{SC}_6\text{H}_5)(\mu\text{-S-CH}_3)(\text{PPh}_3)_3](\text{PF}_6)_2$ (**4**), which arises from intramolecular phosphine displacement by the thio pendant at

Keywords: alkylation • dithiolate • phosphines • platinum • sulfur ligands

the neighboring $\text{SC}_2\text{H}_4\text{SC}_6\text{H}_5$ bridge, has been trapped and characterized. This is an unusual diplatinum complex with three different bridging thio ligands and three different phosphines. The heteroalkylation is screened in situ by ESI-MS, and the resultant spectral data provide a convenient guide for one-pot syntheses of $\{\text{M}_2(\text{SR})(\text{SR}')\}$ from $\{\text{M}_2\text{S}\}$. The isolation and X-ray crystal structure of a homoalkylated analogue $[\text{Pt}_2(\mu\text{-S-CH}_3)_2(\text{PPh}_3)_4](\text{PF}_6)_2$ (**6**) is included for comparison.

Introduction

Transition-metal complexes with doubly bridging thiolates, that is, $(\mu\text{-SR})_2$, are well known,^[1] especially d^8 complexes of $[\text{M}_2(\mu\text{-SR})_2\text{L}_4]$, which have attracted widespread interest with respect to their electronic, structural, and conformational properties.^[2-4] The substituents at the bridging sulfide range from simple alkyl,^[5-8] fluoroalkyl,^[9] phenyl,^[10] fluorinated aryl,^[11] and amino groups^[12] to metal chlorides.^[13] They have been used as synthons for the synthesis of mononuclear Pt^{II} complexes,^[8] for electronics^[14] and catalysis^[7], for the synthesis of vinylthiophenol,^[15] and as models for platinum binding to sulfur-functionalized protein residues.^[16] In almost all cases, both SR thiolato bridges are chemically identical, except that the R groups can be *syn* or *anti*; such orientation would influence the planarity of the $\text{M}(\mu\text{-S})_2\text{M}$

ring.^[2] It is uncertain if the heterogeneity of the bridges would adversely affect the stability, or how it would influence the conformation and activity of the dinuclear framework. These fundamental questions could not be answered experimentally as there is no suitable model for $[\text{Pt}_2(\mu\text{-SR})(\mu\text{-SR}')\text{L}_4]$ ($\text{R} \neq \text{R}'$), nor there is a general method to prepare such complexes. For example, although it is straightforward to prepare $[\text{Pt}_2(\mu\text{-S})(\mu\text{-SR})\text{L}_4]^+$ and $[\text{Pt}_2(\mu\text{-SR})_2\text{L}_4]^{2+}$ from $[\text{Pt}_2(\mu\text{-S})_2\text{L}_4]$ (**1**, $\text{L} = \text{PPh}_3$) through alkylation with RX, this method would not lead to heterodialkylation. All attempts to alkylate $[\text{Pt}_2(\mu\text{-S})(\mu\text{-SR})\text{L}_4]^+$ with $\text{R}'\text{X}$ in which $\text{X} = \text{halide}$ have failed to give the desired compounds, even in the presence of a base such as triethylamine.^[17,18] The failure could be attributed to the exceptionally high stability of $[\text{Pt}_2(\mu\text{-S})(\mu\text{-SR})\text{L}_4]^+$.

Although both sulfur centers in the $\{\text{Pt}_2\text{S}_2\}$ core are highly nucleophilic, upon the attachment of R and transformation to the $\{\text{Pt}_2(\text{S})(\text{SR})\}^+$ core, electron delocalization within the metallo-ring structure and formation of a positively charged monocation discourages further attack of the unsubstituted sulfur atom. Use of strong electrophiles or more forcing conditions only leads to significant decomposition. Dialkylation of both sulfides is possible but only with dihalides having spacer length of up to six carbon atoms between the two alkylating groups,^[17,19] which also results in symmetrical

[a] S. H. Chong, L. L. Koh, T. S. A. Hor
Department of Chemistry, National University of Singapore
3, Science Drive 3
Singapore 117543 (Singapore)
Fax: (+65) 6873-1324
E-mail: andyhor@nus.edu.sg

[b] W. Henderson
Department of Chemistry, University of Waikato
Private Bag 3105, Hamilton (New Zealand)

dithiolates.^[6,20] Reactions with C₁ substrates such as CH₂Cl₂ could lead to dialkylation, which is followed by bridge cleavage and formation of a number of mononuclear and decomposition species.^[21] An alternative approach to start from mononuclear [Pt(SR)(SR')L₂] (with PtL₂²⁺) is also not feasible because there is no simple means to prepare such mixed-thiolato substrates.

Our recent work in the electrospray mass spectrometry (ESI-MS) based survey of the alkylation and arylation of [Pt₂(μ-S)₂(PPh₃)₄] (**1**)^[18] suggested that the outcome of alkylation indeed depends on the strength of the electrophile. The spectral study provided an effective means for us to screen a range of electrophiles and their activities towards **1**. The spectral data thus obtained could then guide us in the bench-top syntheses. We present herein the first successful heterodialkylation of the two bridging sulfides of **1** as a general means to prepare mixed-thiolato bridging complexes. Isolation and crystallographic identification of a number of diplatinum binuclear structures with different thiolate substituents suggested that different chemical entities can be grafted onto the {Pt₂S₂} core.

Results and Discussion

Syntheses and structural studies of heterodialkylation of [Pt₂(μ-S)₂(PPh₃)₄] (**1**)

The reaction of alkyl bromides with **1** occurs rapidly to give the monoalkylated complex [Pt₂(μ-SR)(μ-S)(PPh₃)₄]⁺ (**2**), and the second alkylation is immediately followed by further nucleophilic attack by bromide leading to [Pt₂(μ-SR)₂(PPh₃)₃Br]⁺. However, if the reaction is intercepted upon the formation of **2**, by introducing dimethyl sulfate (Me₂SO₄), a second alkylation on the free sulfide takes place to give the desired heteroalkylation product [Pt₂(μ-SR)(μ-SCH₃)(PPh₃)₄]²⁺ (**3**). Complex **3** represents a new class of diplatinum mixed-thiolate complexes. This is significant in the alkylation and arylation chemistry of [Pt₂(μ-S)₂L₄] complexes in which even a simple derivative such as

[Pt₂(μ-SCH₃)₂(PPh₃)₄]²⁺ has, to date, eluded isolation, although the SCF₃ analogue is known.^[9] Alkylation of other metal systems (such as Mo^[11b-c] and Rh^[1f]) are known but they are beyond the scope of this paper.

By applying such methodology, we were able to synthesize and isolate a series of heterodialkylated platinum sulfide complexes with different R functionalities, including benzyl, allyl, ester, nitrile, and dioxolane (Table 1). The syntheses were prescreened by positive-ion ESI-MS of the reaction mixtures which suggested the formation of positively charged products. Within an hour of adding Me₂SO₄, methylation occurred to give **3**. Addition of NH₄PF₆ gave the corresponding PF₆ salt. The single-crystal X-ray diffraction analyses of the following complexes [Pt₂(μ-SCH₂C₆H₅)(μ-SCH₃)(PPh₃)₄](PF₆)₂ (**3a**), [Pt₂(μ-SCH₂CHCH₂)(μ-SCH₃)(PPh₃)₄](PF₆)₂ (**3b**), and [Pt₂(μ-SC₅H₁₀CO₂CH₂CH₃)(μ-SCH₃)(PPh₃)₄](PF₆)₂ (**3c**) conclusively show the different thiolate bridges in the [Pt₂(SR)(SR')] core. The molecular structures of complexes **3a–c** are shown in Figures 1–3, respectively. Notably, the preparation can be generally applied to systems in which the two thiolato substituents are chemically, electronically, and sterically diverse. For example, one can increase the steric demand of the second substituent (e.g. from CH₃ to CH₂C₆H₅ as in **3a**) or introduce an extended tail structure (e.g. C₅H₁₀CO₂CH₂CH₃ as in **3c**) or an additional functional moiety to the second substituent (such as CN in **3e**, CH₂CHCH₂ in **3b**, and C₂H₄CH(O)₂C₂H₄ in **3f**). The presence of significantly different thiolato residues does not appear to affect the complex stability adversely or their preparation significantly. This illustrates the potential of grafting different organic moieties onto the {Pt₂S₂} core, which is well-known to receive different metal systems. The multipolymetallic chemistry can thus be extended to a rich thiolato chemistry. The central {Pt₂S₂} ring is inevitably folded (with a dihedral angle of 155°, 148°, and 149° for **3a**, **3b**, and **3c**, respectively) and adaptable to different bridge demands. The two thiolate ligands adopt a *syn-exo* conformation, pointing away from the bulky triphenylphosphine groups, which is typical for a bent [M₂(μ-XR)₂L₄] molecule.^[3]

The ³¹P{¹H} NMR spectra of all complexes **3** show a common feature. The two sets of chemically different phosphines, being *trans* to different thiolates, have very similar chemical shifts but different Pt–P couplings. In complex **3a**, two sets of overlapping doublets at δ_p = 19.5 and 19.4 ppm with the associated Pt–P coupling constants ¹J_{Pt–P(1)} = 2924 Hz and ¹J_{Pt–P(2)} = 2974 Hz are observed. The phosphine ligand *trans* to the more-strongly electron-withdrawing μ-SCH₂C₆H₅ should have a higher ¹J_{Pt–P} value of 2974 Hz. The ²J_{P–P} coupling is not defined owing to the overlap of these two doublets. The ³¹P{¹H} NMR spectrum of **3b** shows a similar pattern to that of **3a** with overlapping doublets at δ_p = 19.6 and 19.5 ppm (¹J_{Pt–P(1)} = 2918 Hz and ¹J_{Pt–P(2)} = 2975 Hz). However, for complexes **3c** and **3d**, with the ester thiolate ligand, a broad singlet is observed in each of the spectra: δ_p = 20.3 ppm (¹J_{Pt–P(1)} = 2913 Hz, ¹J_{Pt–P(2)} = 2945 Hz) for **3c** and δ_p = 20.0 ppm (¹J_{Pt–P(1)} = 2923 Hz, ¹J_{Pt–P(2)} =

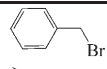
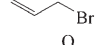
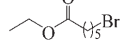
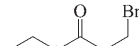
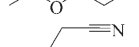
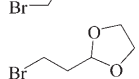
International Advisory Board Member



Andy Hor was born in Hong Kong in 1956. After his BSc(Hons) at Imperial College, London, UK (1979) and his DPhil at Oxford (1983), he carried out postdoctoral studies at Yale Univ., USA (1984). He is Professor and Head of Chemistry of the National Univ. of Singapore and President of the Singapore National Institute of Chemistry. He has published over 180 papers and his numerous awards include a DSc (Univ. of London) and several fellowships and lectureships (Humboldt, Wilsnour, Anthony Mason, etc.).

"I believe that for Chemistry—An Asian Journal to be a premium journal, it needs the collective support of the Asian community. When Asians cooperate, they do it well!"

Table 1. ESI-MS assisted preparation of heterodialkylated platinum sulfide complexes.

RBr	$[\text{Pt}_2(\mu\text{-SR})(\mu\text{-S})(\text{PPh}_3)_4]^+$ (2) (<i>m/z</i>)	$[\text{Pt}_2(\mu\text{-SR})(\mu\text{-SCH}_3)(\text{PPh}_3)_4]^{2+}$ (3) (<i>m/z</i>)
a 	2a (1594)	3a (804)
b 	2b (1544)	3b (779)
c 	2c (1645)	3c (830)
d 	2d (1603)	3d (809.5)
e 	2e (1556)	3e (786)
f 	2f (1604)	3f (809)

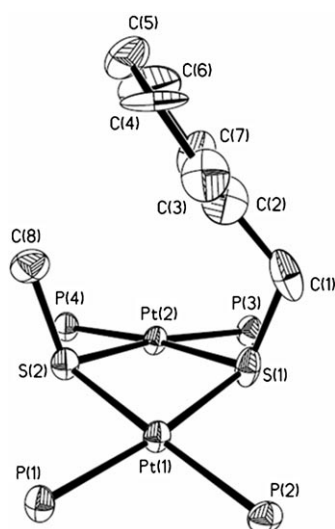


Figure 1. A 50% thermal ellipsoid representation of the cation of $[\text{Pt}_2(\mu\text{-SCH}_2\text{C}_6\text{H}_5)(\mu\text{-SCH}_3)(\text{PPh}_3)_4](\text{PF}_6)_2$ (**3a**). The phenyl rings of PPh_3 and hydrogen atoms are omitted for clarity.

2964 Hz) for **3d**. The different phosphine environments can still be identified from the two sets of $^1J_{\text{Pt-P}}$ values, and the phosphine group *trans* to the more-strongly electron-withdrawing $\mu\text{-SC}_n\text{H}_{2n}\text{CO}_2\text{CH}_2\text{CH}_3$ (**3c**: $n=5$; **3d**: $n=2$) should result in a greater $^1J_{\text{Pt-P}}$ value. The $^{31}\text{P}\{^1\text{H}\}$ NMR spectrum of $[\text{Pt}_2(\mu\text{-SC}_2\text{H}_4\text{CH}(\text{O})_2\text{C}_2\text{H}_4)(\mu\text{-SCH}_3)(\text{PPh}_3)_4](\text{PF}_6)_2$ (**3f**), which bears a dioxolane functionality, displays a multiplet centered at $\delta_{\text{p}}=20.2$ ppm, and the associated satellites for these signals overlap to give a pair of broad satellites resulting in a coupling constant of $^1J_{\text{Pt-P}}=2933$ Hz for the two peaks. Table 2 summarizes the $^{31}\text{P}\{^1\text{H}\}$ NMR results of complexes **3a-f**.

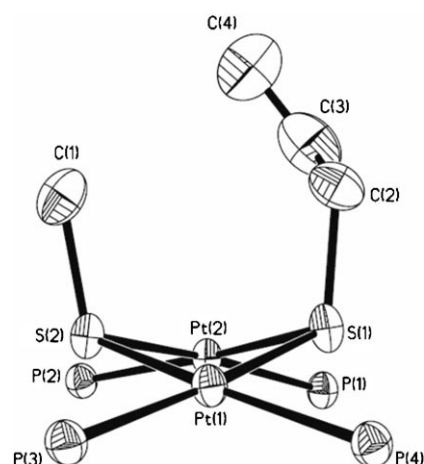


Figure 2. A 50% thermal ellipsoid representation of the cation of $[\text{Pt}_2(\mu\text{-SCH}_2\text{CHCH}_2)(\mu\text{-SCH}_3)(\text{PPh}_3)_4](\text{PF}_6)_2$ (**3b**). The phenyl rings of PPh_3 and hydrogen atoms are omitted for clarity.

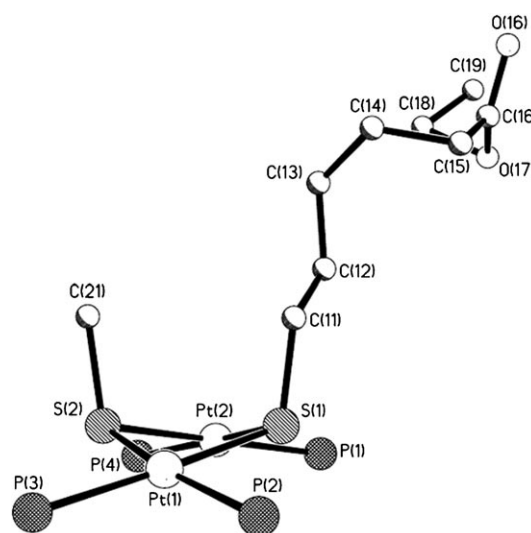


Figure 3. Molecular structure of the cation of $[\text{Pt}_2(\mu\text{-SC}_5\text{H}_{10}\text{CO}_2\text{CH}_2\text{CH}_3)(\mu\text{-SCH}_3)(\text{PPh}_3)_4](\text{PF}_6)_2$ (**3c**). The phenyl rings of PPh_3 and hydrogen atoms are omitted for clarity.

Phosphine displacement in $[\text{Pt}_2(\mu\text{-SR})(\mu\text{-SCH}_3)(\text{PPh}_3)_4]^{2+}$ (**3**)

The reactions of **1** with alkyl halides invariably lead to triphenylphosphine dissociation as a secondary process.^[18,19] The vacated site is usually taken up by the halide (X) resulting in $[\text{Pt}_2(\mu\text{-SRS})(\text{PPh}_3)_3\text{X}]^+$ or $[\text{Pt}_2(\mu\text{-SR})_2(\text{PPh}_3)_3\text{X}]^+$. This problem of phosphine displacement was controlled in this case by the use of Me_2SO_4 , as the resulting methyl sulfate anions are sufficiently non-nucleophilic. However, if R contains a nucleophilic functionality, it could also encourage an intramolecular phosphine displacement. This phenomenon is exemplified in the reaction of 2-bromoethyl phenyl sulfide. The expected heterodialkylated complex is observed with

Table 2. Comparison of $^{31}\text{P}\{^1\text{H}\}$ NMR characteristics for complexes **3a–g**, **4**, and **6**.^[a]

Complex	Solvent	δ ($^{31}\text{P}\{^1\text{H}\}$) [ppm], J [Hz]
3a	CD_2Cl_2	overlapping doublets at $\delta_{\text{p}} = 19.4$ and 19.5 ppm ($^1J_{\text{Pt-P}(1)} = 2924$ Hz, $^1J_{\text{Pt-P}(2)} = 2974$ Hz)
3b	CDCl_3	overlapping doublets at $\delta_{\text{p}} = 19.5$ and 19.6 ppm ($^1J_{\text{Pt-P}(1)} = 2918$ Hz, $^1J_{\text{Pt-P}(2)} = 2975$ Hz)
3c	CD_2Cl_2	broad singlet, $\delta_{\text{p}} = 20.3$ ppm ($^1J_{\text{Pt-P}(1)} = 2913$ Hz, $^1J_{\text{Pt-P}(2)} = 2945$ Hz)
3d	CD_2Cl_2	broad singlet, $\delta_{\text{p}} = 20.0$ ppm ($^1J_{\text{Pt-P}(1)} = 2923$ Hz, $^1J_{\text{Pt-P}(2)} = 2964$ Hz)
3e	CDCl_3	broad singlet, $\delta_{\text{p}} = 18.7$ ppm ($^1J_{\text{Pt-P}(1)} = 2926$ Hz, $^1J_{\text{Pt-P}(2)} = 2979$ Hz)
3f	CD_2Cl_2	multiplet, $\delta_{\text{p}} = 20.2$ ppm ($^1J_{\text{Pt-P}} = 2933$ Hz)
3g	CD_2Cl_2	broad singlet, $\delta_{\text{p}} = 20.0$ ppm ($^1J_{\text{Pt-P}(1)} = 2927$ Hz, $^1J_{\text{Pt-P}(2)} = 2969$ Hz)
4	CD_2Cl_2	3 PPh_3 resonances; doublet of doublets, $\delta_{\text{p}} = 15.3$ – 15.4 ppm ($^1J_{\text{Pt-P}} = 3364$ Hz, $^2J_{\text{P}(1)\text{-P}(2)} = 9$ Hz, $^4J_{\text{P}(2)\text{-P}(3)} = 6$ Hz); broad singlet, $\delta_{\text{p}} = 14.4$ ppm ($^1J_{\text{Pt-P}} = 3142$ Hz); triplet, $\delta_{\text{p}} = 13.3$ ppm ($^1J_{\text{Pt-P}} = 3074$ Hz, $^2J_{\text{P}(1)\text{-P}(2)} = 13$ Hz)
6	CD_2Cl_2	singlet, $\delta_{\text{p}} = 20.4$ ppm ($^1J_{\text{Pt-P}} = 2918$ Hz)

[a] The $^2J_{\text{P-P}}$ coupling constants for complexes **3a**, **3b**, **3f**, and **6** could not be defined.

the loss of one triphenylphosphine group as $[\text{Pt}_2(\mu\text{-SC}_2\text{H}_4\text{SC}_6\text{H}_5)(\mu\text{-SCH}_3)(\text{PPh}_3)_3]^{2+}$ (**4**) in the ESI mass spectrum (m/z 696.5, 100%). In this case, the expected peak for $[\text{Pt}_2(\mu\text{-SC}_2\text{H}_4\text{SC}_6\text{H}_5)(\mu\text{-SCH}_3)(\text{PPh}_3)_3\text{Br}]^+$ (m/z 1473) is absent in the mass spectrum, suggesting that nucleophilic attack from the bromide does not take place. Complex **4** was subsequently isolated as a secondary product in the reaction mixture, which contained primarily **3g**.

Single-crystal X-ray diffraction analyses revealed the expected dinuclear structure of both $[\text{Pt}_2(\mu\text{-SC}_2\text{H}_4\text{SC}_6\text{H}_5)(\mu\text{-SCH}_3)(\text{PPh}_3)_3]^{2+}$ (**4**) (Figure 4) and $[\text{Pt}_2(\mu\text{-SC}_2\text{H}_4\text{SC}_6\text{H}_5)(\mu\text{-SCH}_3)(\text{PPh}_3)_4]^{2+}$ (**3g**) (Figure 5). The former has lost a phosphine group, and the vacant site thus created is taken up by the sulfide of the bridging ethylphenyl thioether. This constitutes an intramolecular ligand substitution driven by a basic pendant (alkylphenyl)sulfide and the formation of a stable five-membered metallo-sulfur ring, which fuses with the $\{\text{Pt}_2\text{S}_2\}$ four-membered ring at the $\text{Pt}(2)\text{-S}(2)$ bond. It gives rise to an unusual diplatinum complex with three different bridging thio ligands and three different phosphine groups. Among the Pt-S bonds, the $\text{Pt}(2)\text{-S}(1)$, which is *trans* to the thio (Ph-S-CH_2) with the weakest *trans* influence, is the shortest (2.295 Å) and presumably strongest. The associated $\text{Pt}(1)\text{-S}(1)$ (2.381 Å) is hence the weakest. The $\text{Pt}(2)\text{-S}(2)$ (2.324(3) Å) and $\text{Pt}(2)\text{-S}(3)$ (2.325(3) Å) are comparable, suggesting that the stronger thiolate sulfur ($\text{S}(2)$) (compared to the thioether $\text{S}(3)$) is offset by its bridging function. These can be reflected in the corresponding Pt-P lengths, for which $\text{Pt}(1)\text{-P}(2)$ is the strongest (2.282(3) Å) and $\text{Pt}(1)\text{-P}(1)$ the weakest (2.300(3) Å), although the differences are not significant. The thiolates $\text{S}(2)$ and $\text{S}(3)$ adopt an *anti* conformation with respect to the $\text{S}(1)$ ligand. The X-ray crystal structure of **3g** (Figure 5) is similar

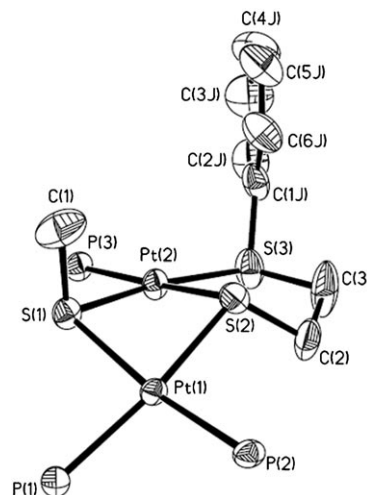


Figure 4. A 50% thermal ellipsoid representation of the cation of $[\text{Pt}_2(\mu\text{-SC}_2\text{H}_4\text{SC}_6\text{H}_5)(\mu\text{-SCH}_3)(\text{PPh}_3)_3](\text{PF}_6)_2$ (**4**). The thiolate ligands adopt an *anti* conformation. The phenyl rings of PPh_3 and hydrogen atoms are omitted for clarity.

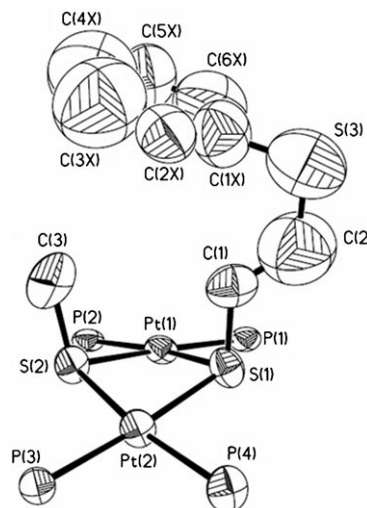


Figure 5. A 50% thermal ellipsoid representation of the molecular structure of $[\text{Pt}_2(\mu\text{-SC}_2\text{H}_4\text{SC}_6\text{H}_5)(\mu\text{-SCH}_3)(\text{PPh}_3)_4]^{2+}$ (**3g**). The phenyl rings of PPh_3 and hydrogen atoms are omitted for clarity.

to that of **3a–c** with a bent $\{\text{Pt}_2\text{S}_2\}$ ring and a dihedral angle of 150° , as well as a *syn-exo* conformation adopted by the two thiolate ligands.

The $^{31}\text{P}\{^1\text{H}\}$ NMR spectrum of **4** in CD_2Cl_2 is consistent with its solid-state structure, giving three distinct resonances at $\delta_{\text{p}} = 15.3$ – 15.4 ppm (dd, $^1J_{\text{Pt-P}} = 3364$ Hz, $^2J_{\text{P}(1)\text{-P}(2)} = 6$ Hz, $^4J_{\text{P}(2)\text{-P}(3)} = 6$ Hz), $\delta_{\text{p}} = 14.4$ ppm (br s, $^1J_{\text{Pt-P}} = 3142$ Hz) and $\delta_{\text{p}} = 13.3$ ppm (t, $^1J_{\text{Pt-P}} = 3074$ Hz, $^2J_{\text{P}(1)\text{-P}(2)} = 13$ Hz). Its spectrum also shows the presence of **3g** (broad singlet at $\delta_{\text{p}} = 20.0$ ppm ($^1J_{\text{Pt-P}(1)} = 2927$ Hz, $^1J_{\text{Pt-P}(2)} = 2969$ Hz)). Complete separation of **4** and **3g** proved to be difficult. ^1H NMR spectroscopic and elemental microanalysis of the sample also suggested the coexistence of **3g** and **4** (observed carbon con-

tent is intermediate (47.76%) between those of **3g** (49.55%) and **4** (44.48%). The ESI spectrum of **3g** gives **4** as the sole peak, suggesting further that **4** is a secondary product of **3g** and that phosphine replacement and ring formation occur readily in solution. When PPh_3 is replaced by a chelating phosphine group such as 1,3-bis(diphenylphosphino)propane (dppp) in a derivative of **1**, that is, $[\text{Pt}_2(\mu\text{-SR})(\mu\text{-S})(\text{dppp})_2]^+$, phosphine displacement can be suppressed, and the formation of $[\text{Pt}_2(\mu\text{-SC}_2\text{H}_4\text{SC}_6\text{H}_5)(\mu\text{-SCH}_3)(\text{dppp})_2]^{2+}$ (**5**) (m/z 715.5, 100%) can be detected in the ESI mass spectrum.

Dimethylation of $[\text{Pt}_2(\mu\text{-S})_2(\text{PPh}_3)_4]$ (**1**)

The results described above suggest that Me_2SO_4 is useful for the methylation of the unreactive sulfide of the monoalkylated complex **2**. Furthermore, the methylsulfate anions generated from Me_2SO_4 are sufficiently non-nucleophilic to stabilize the dicationic dialkylated species. In fact, Me_2SO_4 is powerful enough to result in the dimethylation of complex **1** and hence lead to the isolation of the first dimethylated platinum species, $[\text{Pt}_2(\mu\text{-SCH}_3)_2(\text{PPh}_3)_4][\text{PF}_6]_2$ (**6**) of the type $[\text{Pt}_2(\mu\text{-SR})_2\text{L}_4]$. The $^{31}\text{P}\{^1\text{H}\}$ NMR spectrum of complex **6** in CD_2Cl_2 shows a singlet at $\delta_{\text{P}} = 20.4$ ppm ($^1J_{\text{Pt-P}} = 2918$ Hz) for all four chemically equivalent phosphine groups. Confirmation of its identity by an X-ray diffraction study (Figure 6) shows that the two methylthiolate ligands adopt a *syn-exo* conformation, pointing away from the bulky triphenylphosphine groups. The geometry of the central $[\text{Pt}_2\text{S}_2]$ ring is hinged with a dihedral angle of 157° . The fluoroalkyl derivative $[\text{Pt}_2(\mu\text{-SCF}_3)_2(\text{PPh}_3)_4](\text{BF}_4)_2$, however, has both *syn* and *anti* isomers, as determined by ^{19}F NMR spectroscopic studies, which indicates that the equilibrium between these isomers is not labile under normal conditions.^[9] Its crystal structure has not been reported. A comparison of the metal–thiolate bonds in **6** and **3c** suggest that a long and hindering thiolate tail (as in **3c**) does not lead to any significant weakening (relative to **6**) of the metal–thiolate links: (Pt–S 2.355–2.368(2) Å) in **3c** and Pt–S 2.348–2.366(2) Å in **6**.

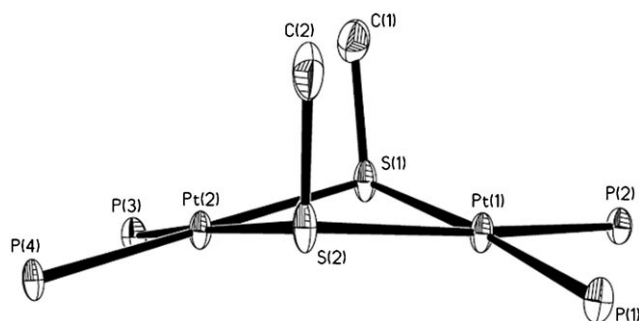


Figure 6. A 50% thermal ellipsoid representation of the cation of $[\text{Pt}_2(\mu\text{-SCH}_3)_2(\text{PPh}_3)_4](\text{PF}_6)_2$ (**6**). The phenyl rings of PPh_3 and hydrogen atoms are omitted for clarity.

Conclusion

Successful and stepwise conversion of sulfide into thiolate and then mixed thiolates has provided a rare and simple route to dinuclear mixed-thiolato complexes, which currently have no established synthetic pathway. The isolation and good stability of diplatinum complexes that carry two hetero bridges of diverse electronic and steric “tails” are somewhat surprising. Its ability to carry functional moieties suggested that we are one step closer to our long-term target of grafting the $[\text{Pt}_2\text{S}_2]$ core onto solid surfaces and developing the “heterogeneous chemistry” of molecular platinum sulfide. We can also apply the heteroalkylation to construct a new series of bridging entities that carry different constituent functionalities for different functions. Since the bridge-cleavage reactions of $[\text{Pt}_2(\mu\text{-SR})_2\text{L}_4]^{2+}$ to $\text{Pt}(\text{SR})_2\text{L}_2$ (+ PtX_2L_2) is known, our method immediately paves a means to prepare mononuclear mixed-dithiolato complexes, which are also difficult to prepare easily by known methods. Full details of such syntheses will be reported in due course.

Experimental Section

Methods and Materials

All manipulations were carried out at room temperature under an atmosphere of dinitrogen. Solvents used were generally analytical grade (Tedia), dried, and deoxygenated before use. Complex **1** was synthesized by metathesis of *cis*- $[\text{PtCl}_2(\text{PPh}_3)_2]$ with $\text{Na}_2\text{S}\cdot 9\text{H}_2\text{O}$ (Riedel–de Haën) in benzene. ESI-MS (80% MeOH, 20% H_2O): $m/z = 1503$ [$M + \text{H}^+$]. The following chemicals were used as supplied from Aldrich: allyl bromide, benzyl bromide, 3-bromopropionitrile, 2-(2-bromoethyl)-1,3-dioxolane, and ammonium hexafluorophosphate. Ethyl 6-bromohexanoate and ethyl 3-bromopropionate were obtained from TCI, 2-bromoethyl phenyl sulfide from Alfa Aesar, and dimethyl sulfate from Merck.

Elemental analyses were performed on a Perkin–Elmer PE 2400 CHNS elemental analyzer. Complexes **3a**, **3b**, **3d**, **3e**, **3g**, and **4** were isolated and analyzed as monohydrates. ^1H NMR and ^{13}C NMR spectra were recorded at 25°C on a Bruker ACF 300 spectrometer (at 300 and 75.47 MHz, respectively) with Me_4Si as internal standard. The ^{31}P NMR spectra were recorded at 25°C at 121.50 MHz with 85% H_3PO_4 as external reference. Electrospray mass spectra were obtained in the positive-ion mode with a Finnigan/MAT LCQ mass spectrometer coupled with a TSP4000 HPLC system and the crystal 310 CE system. The mobile phase was 80% methanol/20% H_2O (flow rate: 0.4 mL min^{-1}). The capillary temperature was 150°C . Peaks were assigned from the m/z values and from the isotope-distribution patterns.

Syntheses

3a: Compound **1** (81.5 mg, 0.054 mmol) was introduced into degassed methanol (35 mL), followed by addition of benzyl bromide (0.10 mL, 144 mg, 0.840 mmol, 15 equiv). The mixture readily changed from an orange suspension to a yellow solution. The solution was left to stir for 1.5 h, followed by the addition of Me_2SO_4 (0.08 mL, 107 mg, 0.846 mmol, 15 equiv). The mixture was stirred for another 2 h, and excess NH_4PF_6 (20.0 mg, 0.123 mmol) was added to the pale yellow solution, which turned into a white suspension. Deionized water (70 mL) was added to induce further precipitation. A white powder was obtained by using vacuum suction filtration and washed with deionized water (100 mL) and diethyl ether (100 mL) to yield **3a** (87.5 mg, 85%). ^1H NMR (300 MHz, CD_2Cl_2): $\delta_{\text{H}} = 0.83$ (br s, 3H; SCH_3), 3.01 (br s, 2H; SCH_2), 6.40–6.43 (m, 5H; C_6H_5), 7.16–7.17 (m, 5H; C_6H_5), 7.25–7.52 ppm (m, 60H; $12\text{C}_6\text{H}_5$); $^{31}\text{P}\{^1\text{H}\}$ NMR (121.5 MHz, CD_2Cl_2): $\delta_{\text{P}} = 19.4$ ppm (d, $^1J_{\text{Pt-P}} = 2974$ Hz),

19.5 (d, $^1J_{\text{Pt-P}}=2924$ Hz); ESI-MS (MeOH/H₂O): m/z (%): 804.4 (100, [M²⁺]); elemental analysis: calcd (%) for Pt₂S₂C₈₀H₇₂OP₆F₁₂ (1917.54): C 50.10, H 3.73, S 3.34; found: C 49.42, H 3.77, S 3.52. Colorless crystals of [Pt₂(μ-SCH₂C₆H₅)(μ-SCH₃)(PPh₃)₄](PF₆)₂ suitable for X-ray crystallographic analysis were obtained from dichloromethane/ethanol (1:1).

3b: A procedure similar to that used above was employed. Allyl bromide (0.02 mL, 28.0 mg, 0.231 mmol, 11 equiv) and **1** (30.7 mg, 0.020 mmol) in methanol (15 mL) gave a yellow solution after 10 min. The mixture was stirred for 1.5 h, and then Me₂SO₄ (0.03 mL, 40.0 mg, 0.317 mmol, 15 equiv) was added, and the solution was stirred for 2 h. Excess NH₄PF₆ (15.0 mg, 0.092 mmol) was added into the colorless solution, readily turning it into a white suspension. Deionized water (40 mL) was used to complete precipitation. The white precipitate of **3b** (32.8 mg, 89%) obtained by using vacuum suction filtration was washed with deionized water (100 mL) and diethyl ether (100 mL). ¹H NMR (300 MHz, CD₂Cl₂): δ_H=0.89 (br s, 3H; SCH₃), 2.53 (br s, 2H; SCH₂), 4.85–4.91 (m, 1H; SCH₂CH), 4.44–4.53 (m, 1H; CHCH₂H_b), 4.85 (br s, 1H; CHCH₂H_b), 7.20–7.50 ppm (m, 60H; 12C₆H₅); ³¹P{¹H} NMR (121.5 MHz, CDCl₃): δ_P=19.5 ppm (d, $^1J_{\text{Pt-P}}=2975$ Hz), 19.6 (d, $^1J_{\text{Pt-P}}=2918$ Hz); ESI-MS (MeOH/H₂O): m/z (%): 779.0 (100, [M²⁺]); elemental analysis: calcd (%) for Pt₂S₂C₇₆H₇₀OP₆F₁₂ (1867.48): C 48.90, H 3.72, S 3.43; found: C 48.91, H 3.71, S 3.42. Colorless crystals of [Pt₂(μ-SCH₂CHCH₂)(μ-SCH₃)(PPh₃)₄](PF₆)₂ suitable for X-ray crystallographic analysis were obtained from dichloromethane/ethanol (1:1).

3c: Complex **1** (41.4 mg, 0.028 mmol) was introduced into degassed methanol (15 mL) followed by the addition of ethyl 6-bromohexanoate (60.6 mg, 0.272 mmol, 10 equiv). The mixture was stirred for 2.5 h, Me₂SO₄ (0.03 mL, 40.0 mg, 0.317 mmol, 11 equiv) was added, and the yellow solution was decolorized after 2 h. Excess NH₄PF₆ (15.0 mg, 0.092 mmol) was then added, resulting in a white suspension. Deionized water (40 mL) was used to complete precipitation. The white precipitate of **3c** (38.0 mg, 71%) obtained by vacuum suction filtration was washed with deionized water (100 mL) and diethyl ether (100 mL). ¹H NMR (300 MHz, CD₂Cl₂): δ_H=0.89 (br s, 3H; SCH₃), 0.84 (t, $J=7$ Hz, 2H; SCH₂), 1.22–1.29 (m, 2H; SCH₂CH₂), 1.11–1.20 (m, 2H; SCH₂CH₂CH₂), 2.06–2.11 (m, 2H; CH₂CH₂CO), 2.19 (br s, 2H; CH₂CO), 4.09–4.16 (q, $J=7$ Hz, 2H; OCH₂), 1.26 (t, $J=7$ Hz, 3H; OCH₂CH₃), 7.21–7.47 ppm (m, 60H; 12C₆H₅); ¹³C NMR (75.47 MHz, CD₂Cl₂): δ_C=14.4, 16.4, 24.5, 28.2, 32.1, 34.0, 35.8, 60.5, 126.8, 129.4, 132.6, 134.6, 173.6 ppm; ³¹P{¹H} NMR (121.5 MHz, CD₂Cl₂): δ_P=20.3 (br s, $^1J_{\text{Pt-P(1)}}=2913$ Hz, $^1J_{\text{Pt-P(2)}}=2945$ Hz); ESI-MS (MeOH/H₂O): m/z (%): 830.3 (100, [M²⁺]); elemental analysis: calcd (%) for Pt₂S₂C₈₁H₇₆O₂P₆F₁₂ (1949.58): C 49.90, H 3.93, S 3.29; found: C 49.56, H 4.19, S 3.22. Colorless crystals of [Pt₂(μ-SC₅H₁₀CO₂CH₂CH₃)(μ-SCH₃)(PPh₃)₄](PF₆)₂ suitable for X-ray crystallographic analysis were obtained from dichloromethane/benzene (2:1).

3d: Complex **1** (50.0 mg, 0.033 mmol) was introduced into degassed methanol (25 mL) followed by the addition of ethyl 3-bromopropionate (0.05 mL, 63.0 mg, 0.348 mmol, 10 equiv). The mixture was stirred for 2 h, and then Me₂SO₄ (0.05 mL, 66.7 mg, 0.528 mmol, 16 equiv) was added to the yellow solution and stirred for a further 1.5 h. Excess NH₄PF₆ (15.0 mg, 0.092 mmol) was then added, resulting in a white suspension. Deionized water (50 mL) was used to complete precipitation. The white precipitate of **3d** (55.2 mg, 87%) obtained by vacuum suction filtration was washed with deionized water (100 mL) and diethyl ether (100 mL). ¹H NMR (300 MHz, CD₂Cl₂): δ_H=0.92 (br s, 3H; SCH₃), 0.58 (t, $J=7$ Hz, 2H; SCH₂), 2.56 (br s, 2H; CH₂CO), 4.04–4.11 (q, $J=7$ Hz, 2H; OCH₂), 1.22 (t, $J=7$ Hz, 3H; OCH₂CH₃), 7.20–7.50 ppm (m, 60H; 12C₆H₅); ¹³C NMR (75.47 MHz, CD₂Cl₂): δ_C=14.2, 16.3, 29.7, 33.6, 61.2, 126.7, 129.4, 132.6, 134.6, 170.9 ppm; ³¹P{¹H} NMR (121.5 MHz, CD₂Cl₂): δ_P=20.0 ppm (br s, $^1J_{\text{Pt-P(1)}}=2923$ Hz, $^1J_{\text{Pt-P(2)}}=2964$ Hz); ESI-MS (MeOH/H₂O): m/z (%): 809.5 (100, [M²⁺]); elemental analysis: calcd (%) for Pt₂S₂C₇₈H₇₄O₂P₆F₁₂ (1927.53): C 48.60, H 3.87, S 3.33; found: C 48.63, H 3.92, S 3.22.

3e: 3-bromopropionitrile (0.03 mL, 48.5 mg, 0.362 mmol, 12 equiv) and complex **1** (44.6 mg, 0.030 mmol) in degassed methanol (20 mL) gave a yellow solution after 10 min. The mixture was stirred for 1.5 h, Me₂SO₄ (0.04 mL, 53.3 mg, 0.423 mmol, 15 equiv) was added, and the solution was stirred for a further 1.5 h. Excess NH₄PF₆ (20.0 mg, 0.123 mmol) was

added to the pale yellow solution, turning it into a suspension. Deionized water (40 mL) was added to complete the precipitation. The pale yellow precipitate of **3e** (50.6 mg, 92%) obtained by vacuum suction filtration was washed with deionized water (100 mL) and diethyl ether (100 mL). ¹H NMR (300 MHz, CD₂Cl₂): δ_H=0.91 (br s, 3H; SCH₃), 0.65 (br s, 2H; SCH₂), 2.43 (br s, 2H; CH₂CN), 7.26–7.51 ppm (m, 60H; 12C₆H₅); ¹³C NMR (75.47 MHz, CD₂Cl₂): δ_C=16.7, 18.0, 30.5, 118.7, 126.2, 129.4, 132.8, 134.7 ppm; ³¹P{¹H} NMR (121.5 MHz, CDCl₃): δ_P=18.7 ppm (br s, $^1J_{\text{Pt-P(1)}}=2926$ Hz, $^1J_{\text{Pt-P(2)}}=2979$ Hz); ESI-MS (MeOH/H₂O): m/z (%): 786.0 (100, [M²⁺]); elemental analysis: calcd (%) for Pt₂S₂C₇₆H₆₈NOP₆F₁₂ (1880.48): C 48.54, H 3.70, S 3.41, N 0.74; found: C 48.55, H 3.58, S 3.26, N 0.71.

3f: Complex **1** (44.5 mg, 0.030 mmol) was introduced into degassed methanol (20 mL) followed by the addition of 2-(2-bromoethyl)-1,3-dioxolane (0.03 mL, 46.3 mg, 0.256 mmol, 9 equiv). The mixture was stirred overnight to yield a yellow solution. Me₂SO₄ (0.03 mL, 40.0 mg, 0.317 mmol, 11 equiv) was then added, and the solution was stirred for a further 1.5 h. Excess NH₄PF₆ (20.0 mg, 0.123 mmol) was added to the pale yellow solution, turning it into a suspension. Deionized water (40 mL) was added to complete the precipitation. The pale yellow precipitate of **3f** (42.3 mg, 75%) obtained by vacuum suction filtration was washed with deionized water (100 mL) and diethyl ether (100 mL). ¹H NMR (300 MHz, CD₂Cl₂): δ_H=0.86 (br s, 3H; SCH₃), 2.20–2.31 (m, 4H; SCH₂CH₂), 4.39 (t, $J=4$ Hz, 1H; CH₂CH(O)₂), 3.77–3.81 (m, 4H; OCH₂CH₂O), 7.24–7.48 ppm (m, 60H; 12C₆H₅); ¹³C NMR (75.47 MHz, CD₂Cl₂): δ_C=16.2, 30.3, 35.3, 65.3, 101.8, 126.7, 129.5, 132.7, 134.5 ppm; ³¹P{¹H} NMR (121.5 MHz, CD₂Cl₂): δ_P=20.2 ppm (m, $^1J_{\text{Pt-P}}=2933$ Hz); ESI-MS (MeOH/H₂O): m/z (%): 809.4 (100, [M²⁺]); elemental analysis: calcd (%) for Pt₂S₂C₇₈H₇₂O₂P₆F₁₂ (1909.52): C 49.02, H 3.80, S 3.36; found: C 48.78, H 3.79, S 3.03.

3g and 4: Complex **1** (40.7 mg, 0.027 mmol) was introduced into degassed acetone (18 mL) followed by the addition of 2-bromoethyl phenyl sulfide (48.2 mg, 0.222 mmol, 8 equiv). The mixture was stirred for 1.75 h to yield a yellow solution. Me₂SO₄ (0.02 mL, 26.7 mg, 0.211 mmol, 8 equiv) was then added, and the solution was stirred overnight. Excess NH₄PF₆ (20.0 mg, 0.123 mmol) was added to the faint yellow solution, turning it into a suspension. Deionized water (40 mL) was added to complete the precipitation. The white precipitate (39.6 mg, 87%) obtained by vacuum suction filtration was washed with deionized water (100 mL) and diethyl ether (100 mL). ¹H NMR (300 MHz, CD₂Cl₂): δ_H=0.61 (br s, 3H; SCH₃ of **3g**), 1.07 (t, $J=8$ Hz, 2H; SCH₂CH₂S of **3g**), 2.19 (br s, 2H; SCH₂CH₂S of **3g**), 1.61–1.67 (m, 4H; SCH₂CH₂S of **4**), 7.09–7.44 ppm (m, 115H; 23C₆H₅ of **3g** and **4**); ³¹P{¹H} NMR (121.5 MHz, CD₂Cl₂): δ_P=20.0 ppm (br s, $^1J_{\text{Pt-P(1)}}=2927$ Hz, $^1J_{\text{Pt-P(2)}}=2969$ Hz) for **3g**; δ_P=15.3–15.4 (dd, $^1J_{\text{Pt-P}}=3364$ Hz, $^2J_{\text{P(1)-P(2)}}=9$ Hz, $^4J_{\text{P(2)-P(3)}}=6$ Hz), δ_P=14.4 (br s, $^1J_{\text{Pt-P}}=3142$ Hz), 13.3 ppm (t, $^1J_{\text{Pt-P}}=3074$ Hz, $^2J_{\text{P(1)-P(2)}}=13$ Hz) for **4**; ESI-MS (MeOH/H₂O): m/z (%): 696.2 (100) for **4**. Colorless crystals suitable for X-ray analysis were obtained from dichloromethane/benzene (1:1).

6: Excess Me₂SO₄ (0.02 mL, 26.7 mg, 0.211 mmol, 10 equiv) was introduced into an orange solution of **1** (39.4 mg, 0.026 mmol) in methanol (18.0 mL). The solution was mixed for 2 h, and excess NH₄PF₆ (15.0 mg, 0.092 mmol) was added to the pale yellow solution, which was then stirred for a further 1 h to give a white suspension. Deionized water (40 mL) was added to complete precipitation. The product obtained by vacuum suction filtration was washed with deionized water (100 mL) and diethyl ether (100 mL) to give **6** (43.7 mg, 91%) as a white powder. ¹H NMR (300 MHz, CD₂Cl₂): δ_H=1.02 (br s, 6H; 2 SCH₃), 7.23–7.49 (m, 60H; 12C₆H₅); ³¹P{¹H} NMR (121.5 MHz, CD₂Cl₂): δ_P=20.4 ppm (s, $^1J_{\text{Pt-P}}=2918$ Hz); ESI-MS (MeOH/H₂O): m/z (%): 766.2 (100, [M²⁺]); elemental analysis: calcd (%) for Pt₂S₂C₇₄H₆₆P₆F₁₂ (1823.43): C 48.74, H 3.65, S 3.52; found: C 48.26, H 3.43, S 3.79. Colorless crystals of [Pt₂(μ-SCH₃)₂(PPh₃)₄](PF₆)₂ suitable for X-ray analysis were obtained from dichloromethane/methanol (1:1).

X-ray Crystal-Structure Determination and Refinement

Selected bond lengths and angles for **3a–c**, **3g**, **4**, and **6** are given in Table 3. All measurements were made at 223 K on a Bruker AXS SMART APEX diffractometer equipped with a CCD area detector by

Table 3. Selected bond lengths (Å) and angles (°) for complexes.

3a					
Pt(1)–P(1)	2.302(3)	Pt(1)–S(2)	2.368(3)	S(2)–C(8)	1.838(14)
Pt(1)–P(2)	2.293(3)	Pt(2)–S(1)	2.367(3)	S(1)–C(1)	1.843(15)
Pt(1)–S(1)	2.354(3)	Pt(2)–S(2)	2.350(3)		
Pt(1)–S(1)–Pt(2)	95.02(11)	P(1)–Pt(1)–S(1)	168.94(11)	C(1)–S(1)–Pt(1)	107.8(4)
Pt(1)–S(2)–Pt(2)	95.09(11)	P(1)–Pt(1)–S(2)	87.58(11)	C(1)–S(1)–Pt(2)	113.4(4)
S(1)–Pt(1)–S(2)	81.79(10)	P(2)–Pt(1)–S(1)	92.38(11)	C(8)–S(2)–Pt(1)	113.8(4)
P(1)–Pt(1)–P(2)	97.90(12)	P(2)–Pt(1)–S(2)	172.11(12)	C(8)–S(2)–Pt(2)	108.8(4)
3b					
Pt(1)–P(3)	2.288(2)	Pt(1)–S(2)	2.356(2)	S(2)–C(1)	1.835(11)
Pt(1)–P(4)	2.308(2)	Pt(2)–S(1)	2.360(2)	S(1)–C(2)	1.847(11)
Pt(1)–S(1)	2.376(2)	Pt(2)–S(2)	2.377(2)		
Pt(1)–S(1)–Pt(2)	92.75(8)	P(3)–Pt(1)–S(1)	175.33(8)	C(2)–S(1)–Pt(1)	108.1(4)
Pt(1)–S(2)–Pt(2)	92.84(7)	P(3)–Pt(1)–S(2)	93.34(8)	C(2)–S(1)–Pt(2)	104.2(3)
S(1)–Pt(1)–S(2)	82.16(7)	P(4)–Pt(1)–S(1)	87.49(8)	C(1)–S(2)–Pt(1)	104.8(3)
P(3)–Pt(1)–P(4)	97.08(8)	P(4)–Pt(1)–S(2)	168.85(8)	C(1)–S(2)–Pt(2)	110.3(4)
3c					
Pt(1)–P(3)	2.289(2)	Pt(1)–S(2)	2.344(2)	S(2)–C(21)	1.863(15)
Pt(1)–P(2)	2.302(2)	Pt(2)–S(1)	2.355(2)	S(1)–C(11)	1.828(16)
Pt(1)–S(1)	2.368(2)	Pt(2)–S(2)	2.365(2)		
Pt(1)–S(1)–Pt(2)	93.28(8)	P(3)–Pt(1)–S(1)	173.98(8)	C(11)–S(1)–Pt(1)	106.9(5)
Pt(1)–S(2)–Pt(2)	93.64(8)	P(3)–Pt(1)–S(2)	92.13(8)	C(11)–S(1)–Pt(2)	106.7(4)
S(1)–Pt(1)–S(2)	81.89(8)	P(2)–Pt(1)–S(1)	87.26(8)	C(21)–S(2)–Pt(1)	105.3(4)
P(2)–Pt(1)–P(3)	98.68(8)	P(2)–Pt(1)–S(2)	168.83(8)	C(21)–S(2)–Pt(2)	106.0(5)
3g					
Pt(1)–P(1)	2.273(5)	Pt(1)–S(2)	2.356(5)	S(2)–C(3)	1.88(3)
Pt(1)–P(2)	2.297(5)	Pt(2)–S(1)	2.360(5)	S(1)–C(1)	1.74(2)
Pt(1)–S(1)	2.345(5)	Pt(2)–S(2)	2.354(4)		
Pt(1)–S(1)–Pt(2)	93.82(17)	P(1)–Pt(1)–S(1)	93.24(17)	C(1)–S(1)–Pt(1)	104.4(8)
Pt(1)–S(2)–Pt(2)	93.67(18)	P(1)–Pt(1)–S(2)	175.12(15)	C(1)–S(1)–Pt(2)	104.2(9)
S(1)–Pt(1)–S(2)	81.95(17)	P(2)–Pt(1)–S(1)	169.13(18)	C(3)–S(2)–Pt(1)	109.7(8)
P(1)–Pt(1)–P(2)	97.38(17)	P(2)–Pt(1)–S(2)	87.39(17)	C(3)–S(2)–Pt(2)	103.9(6)
4					
Pt(1)–P(1)	2.300(3)	Pt(1)–S(2)	2.361(3)	S(1)–C(1)	1.811(14)
Pt(1)–P(2)	2.282(3)	Pt(2)–S(1)	2.295(3)	S(2)–C(2)	1.834(13)
Pt(2)–P(3)	2.288(3)	Pt(2)–S(2)	2.324(3)	S(3)–C(3)	1.837(13)
Pt(1)–S(1)	2.381(3)	Pt(2)–S(3)	2.325(3)	S(3)–C(1J)	1.766(14)
Pt(1)–S(1)–Pt(2)	90.03(10)	P(1)–Pt(1)–S(1)	88.37(10)	C(2)–S(2)–Pt(1)	111.2(5)
Pt(1)–S(2)–Pt(2)	89.81(10)	P(1)–Pt(1)–S(2)	165.80(10)	C(2)–S(2)–Pt(2)	97.9(4)
S(1)–Pt(1)–S(2)	80.07(10)	P(2)–Pt(1)–S(1)	169.45(10)	C(3)–S(3)–Pt(2)	103.0(5)
S(2)–Pt(2)–S(3)	88.13(11)	P(2)–Pt(1)–S(2)	94.85(10)	C(3)–S(3)–C(1J)	102.6(7)
P(1)–Pt(1)–P(2)	97.85(10)	C(1)–S(1)–Pt(1)	102.5(5)		
P(3)–Pt(2)–S(3)	96.03(11)	C(1)–S(1)–Pt(2)	102.2(5)		
6					
Pt(1)–P(1)	2.281(2)	Pt(1)–S(2)	2.348(2)	S(1)–C(1)	1.814(8)
Pt(1)–P(2)	2.299(2)	Pt(2)–S(1)	2.352(2)	S(2)–C(2)	1.809(8)
Pt(1)–S(1)	2.366(2)	Pt(2)–S(2)	2.366(2)		
Pt(1)–S(1)–Pt(2)	95.28(5)	P(1)–Pt(1)–P(2)	96.69(5)	C(1)–S(1)–Pt(1)	109.4(2)
Pt(1)–S(2)–Pt(2)	95.39(5)	P(1)–Pt(1)–S(1)	173.81(5)	C(1)–S(1)–Pt(2)	101.7(2)
S(1)–Pt(1)–S(2)	82.07(5)	P(1)–Pt(1)–S(2)	92.09(5)		

ical absorption correction; and SHELXTL^[24] was used for space-group and structure determination, refinements, graphics, and structure reporting. The structure was refined by full-matrix least squares on F^2 with anisotropic thermal parameters for non-hydrogen atoms. A summary of crystallographic parameters for the data collections and refinements is given in Table 4. For **3a**, there are disordered solvent molecules of dichloromethane, which explains the high R values. There are four dichloromethane molecules, with three and two halves at special positions. The titled cation is disordered, with the two substituted SR groups switching positions. One of the three chloroform solvent molecules is disordered in **3b**, and there is one molecule of ethanol in the asymmetric unit as well. For **3c**, the asymmetric unit contains 2.5 molecules of dichloromethane and half of a molecule of benzene. The two substituted SR groups switch positions (50:50), causing disorder in the crystal packing. The atoms of these disordered parts were located from difference maps. Restraints in bond lengths and thermal parameters were applied during least-squares refinement. Crystals of **3g** and **4** were obtained from the same crop of sample. For **3g**, some atoms did not behave well on refinement, and some benzene rings were refined as hexagons. Restraints in distances and thermal parameters were applied. The atoms of the $C_7H_4SC_6H_5$ chain had very high thermal parameters and the possibility of disorder for this chain could not be ruled out. For **4**, there are 1.5 dichloromethane molecules, one of which was assigned less weight to give more realistic thermal parameters. This is probably the result of the crystal losing solvent. For **6**, the structure was solved by using Patterson methods and developed normally. There are five dichloromethane molecules of solvation in the asymmetric unit, reasonably well-ordered by H-bonding interactions to the PF_6^- anions. CCDC-292463 (**3a**), 292464 (**3b**), 299556 (**3c**), 299557 (**3g**), 299558 (**4**), 292465 (**6**) contain the supplementary crystallographic data for this paper. These data can be obtained free of charge via www.ccdc.cam.ac.uk/conts/retrieving.html (or from the Cambridge Crystallographic Data Centre, 12, Union Road, Cambridge CB21EZ, UK; fax: (+44)1223-336-033; or deposit@ccdc.cam.ac.uk).

using MoK_{α} radiation ($\lambda = 0.71073 \text{ \AA}$). The software SMART^[22] was used for the collection of data frames, for indexing reflections, and to determine lattice parameters; SAINT^[22] was used for the integration of the intensity of the reflections and for scaling; SADABS^[23] was used for empir-

Table 4. Crystallographic data for complexes **3a–c**, **3g**, **4** and **6**.

	3a ·4 CH ₂ Cl ₂	3b ·3 CHCl ₃ ·CH ₃ CH ₂ OH	3c ·2.5 CH ₂ Cl ₂ ·0.5 C ₆ H ₆	3g ·2.5 CH ₂ Cl ₂	4 ·1.5 CH ₂ Cl ₂	6 ·5 CH ₂ Cl ₂
Formula	C ₈₄ H ₇₈ Cl ₈ F ₁₂ P ₆ Pt ₂ S ₂	C ₈₁ H ₇₇ Cl ₉ F ₁₂ OP ₆ Pt ₂ S ₂	C _{86.5} H ₈₆ Cl ₅ F ₁₂ O ₂ P ₆ Pt ₂ S ₂	C _{83.5} H ₇₇ Cl ₅ F ₁₂ P ₆ Pt ₂ S ₃	C _{64.5} H ₆₀ Cl ₃ F ₁₂ P ₃ Pt ₂ S ₃	C ₇₉ H ₇₆ Cl ₁₀ F ₁₂ P ₆ Pt ₂ S ₂
<i>M</i>	2239.18	2253.60	2202.92	2157.88	1810.68	2248.02
Crystal system	Monoclinic	Triclinic	Triclinic	Triclinic	Triclinic	Triclinic
Space group	<i>P</i> 2 ₁ / <i>n</i>	<i>P</i> -1	<i>P</i> -1	<i>P</i> -1	<i>P</i> -1	<i>P</i> -1
<i>a</i> [Å]	17.674(7)	13.5729(5)	14.0271(9)	13.703(5)	12.8474(6)	15.2565(11)
<i>b</i> [Å]	23.1955(11)	13.9237(5)	17.4988(12)	17.616(6)	13.8941(6)	17.1975(13)
<i>c</i> [Å]	21.027(9)	23.4082(9)	18.5464(13)	18.518(7)	21.9957(10)	17.5644(12)
<i>α</i> [°]	90	91.463(10)	93.175(10)	85.253(5)	76.831(10)	76.565(10)
<i>β</i> [°]	91.221(10)	92.302(10)	100.76(10)	79.413(5)	80.505(10)	79.809(10)
<i>γ</i> [°]	90	98.881(10)	90.17(10)	86.655(5)	65.853(10)	73.309(10)
<i>V</i> [Å ³]	8618.2(6)	4365.0(3)	4465.0(5)	4375(3)	3477.1(3)	4236.3(5)
<i>Z</i>	4	2	2	2	2	2
<i>ρ</i> _{calcd} [g cm ⁻³]	1.726	1.715	1.639	1.638	1.729	1.751
<i>μ</i> [mm ⁻¹]	3.721	3.705	3.505	3.597	4.410	3.822
<i>T</i> [K]	223(2)	203(2)	223(2)	223(2)	223(2)	113(2)
Reflections measured	49860	58130	47506	37690	45998	34795
Independent reflections	15170	20006	15725	15375	15946	16548
<i>R</i> _{int}	0.1217	0.0899	0.0578	0.1320	0.0772	0.0336
Parameters	1036	1022	995	975	821	1002
<i>R</i> (<i>F</i> , <i>F</i> ² > 2σ)	0.0797	0.0676	0.0589	0.0954	0.0835	0.0521
<i>R</i> _w (<i>F</i> ² , all data)	0.1383	0.1046	0.0950	0.1853	0.1128	0.0664
Goodness of fit on <i>F</i> ²	1.066	1.031	1.054	0.993	1.159	1.032
Max., min. electron density [e Å ⁻³]	2.033, -2.073	2.354, -1.827	4.243, -1.247	2.757, -2.311	4.763, -3.391	5.139, -3.930

Acknowledgements

We acknowledge the National University of Singapore for financial support, and S.H.C. thanks the NUS for a Kiang Ai Kim Graduate Research Scholarship. We are grateful to L. L. Koh and G. K. Tan for assistance with X-ray crystallographic data collection and analysis for **3a–c**, **3g**, and **4**, and Professor Ward Robinson (University of Canterbury) for **6**. We thank Professor Brian Nicholson for solving the X-ray crystal structure of **6**, and for helpful discussions. W.H., S.H.C., and T.S.A.H. thank the Asia:NZ Foundation for a grant.

- [1] a) P. J. Blower, J. R. Dilworth, *Coord. Chem. Rev.* **1987**, *76*, 121; b) L. D. Vasquez, B. C. Noll, M. R. DuBois, *Inorg. Chem.* **2001**, *40*, 1391; c) J. GaBay, S. Dietz, P. Bernatis, M. R. DuBois, *Organometallics* **1993**, *12*, 3630; d) L. L. Lopez, P. Bernatis, J. Birnbaum, R. C. Haltiwanger, M. R. DuBois, *Organometallics* **1992**, *11*, 2424; e) L. D. Tanner, R. C. Haltiwanger, J. Noordik, M. R. DuBois, *Inorg. Chem.* **1988**, *27*, 1736; f) H. Song, R. C. Haltiwanger, M. R. DuBois, *Organometallics* **1987**, *6*, 2021.
- [2] M. Capdevila, W. Clegg, P. González-Duarte, A. Jarid, A. Lledós, *Inorg. Chem.* **1996**, *35*, 490.
- [3] G. Aullón, G. Ujaque, A. Lledós, S. Alvarez, *Chem. Eur. J.* **1999**, *5*, 1391.
- [4] M. Capdevila, P. González-Duarte, C. Foces-Foces, F. Cano, M. Martínez-Ripoll, *J. Chem. Soc. Dalton Trans.* **1990**, 143.
- [5] M. C. Hall, J. A. J. Jarvis, B. T. Kilbourn, P. G. Owston, *J. Chem. Soc. Dalton Trans.* **1972**, 1544.
- [6] C. E. Briant, C. J. Gardner, T. S. A. Hor, N. D. Howells, D. M. P. Mingos, *J. Chem. Soc. Dalton Trans.* **1984**, 2645.
- [7] H. C. Clark, V. K. Jain, G. S. Rao, *J. Organomet. Chem.* **1985**, *279*, 181.
- [8] M. R. Plutino, L. M. Sclaro, A. Albinati, R. Romeo, *J. Am. Chem. Soc.* **2004**, *126*, 6470.
- [9] K. R. Dixon, K. C. Moss, M. A. R. Smith, *J. Chem. Soc. Dalton Trans.* **1974**, 971.
- [10] a) E. M. Padilla, J. A. Golden, P. N. Richmann, C. M. Jensen, *Polyhedron* **1991**, *10*, 1343; b) V. K. Jain, S. Kannan, R. J. Butcher, J. P. Jasinski, *J. Organomet. Chem.* **1994**, *468*, 285; c) I. Nakanishi, S. Tanaka, K. Matsumoto, S. Ooi, *Acta Crystallogr. Sect. C* **1994**, *50*, 58.
- [11] a) R. H. Fenn, G. R. Segrott, *J. Chem. Soc. A* **1970**, 3197; b) R. H. Fenn, G. R. Segrott, *J. Chem. Soc. Dalton Trans.* **1972**, 330; c) L. Villanueva, M. Arroyo, S. Bernès, H. Torrens, *Chem. Commun.* **2004**, 1942.
- [12] M. Capdevila, W. Clegg, P. González-Duarte, B. Harris, I. Mira, J. Sola, I. C. Taylor, *J. Chem. Soc. Dalton Trans.* **1992**, 2817.
- [13] a) W. Bos, J. J. Bour, P. P. J. Schlebos, P. Hageman, W. P. Bosman, J. J. M. Smits, J. A. C. van Wietmarschen, P. T. Beurskens, *Inorg. Chim. Acta* **1986**, *119*, 141; b) H. Liu, A. L. Tan, C. R. Cheng, K. F. Mok, T. S. A. Hor, *Inorg. Chem.* **1997**, *36*, 2916; c) Z. Li, S.-W. A. Fong, J. S. L. Yeo, W. Henderson, K. F. Mok, T. S. A. Hor, in *Modern coordination chemistry: the legacy of Joseph Chatt* (Eds.: G. J. Leigh and N. Winterton), Royal Society of Chemistry, Cambridge, **2002**, p. 355.
- [14] a) S. Dey, V. K. Jain, S. Chaudhury, A. Knoedler, F. Lissner, W. Kaim, *J. Chem. Soc. Dalton Trans.* **2001**, 723; b) A. Singhal, V. K. Jain, A. Klein, M. Niemeyer, W. Kaim, *Inorg. Chim. Acta* **2004**, *357*, 2134.
- [15] J. J. Garcia, A. Arevalo, V. Montiel, F. D. Rio, B. Quiroz, H. Adams, P. M. Maitlis, *Organometallics* **1997**, *16*, 3216.
- [16] a) K. A. Mitchell, K. C. Streveler, C. M. Jensen, *Inorg. Chem.* **1993**, *32*, 2608; b) K. A. Mitchell, C. M. Jensen, *Inorg. Chem.* **1995**, *34*, 4441; c) K. A. Mitchell, C. M. Jensen, *Inorg. Chim. Acta* **1997**, *265*, 103.
- [17] T. S. A. Hor, unpublished results.
- [18] W. Henderson, S. H. Chong and T. S. A. Hor, *Inorg. Chim. Acta* in press.

- [19] a) S. H. Chong, A. Tjindrawan, T. S. A. Hor, *J. Mol. Catal. A* **2003**, 204, 267; b) S. H. Chong, D. J. Young, T. S. A. Hor, *J. Organomet. Chem.* **2005**, 691, 349.
- [20] a) J. Chatt, F. A. Hart, *J. Chem. Soc.* **1960**, 2807; b) P. H. Bird, U. Sirwardane, R. D. Lai, A. Shaver, *Can. J. Chem.* **1982**, 60, 2075.
- [21] a) S. W. A. Fong and T. S. A. Hor, *J. Chem. Soc. Dalton Trans.* **1999**, 639 and refs therein; b) R. Mas-Ballesté, M. Capdevila, P. A. Champkin, W. Clegg, R. A. Coxall, A. Lledós, C. Mégret, P. González-Duarte, *Inorg. Chem.* **2002**, 41, 3218; c) P. González-Duarte, A. Lledós and R. Mas-Ballesté, *Eur. J. Inorg. Chem.* **2004**, 3585.
- [22] SMART & SAINT Software Reference Manuals, version 4.0, Siemens Energy & Automation, Inc., Analytical Instrumentation, Madison, WI, **1996**.
- [23] G. M. Sheldrick, SADABS, a software for empirical adsorption correction, University of Göttingen, Göttingen, **1993**.
- [24] G. M. Sheldrick, SHELXTL, VERSION 5.03, Siemens Energy & Automation, Inc., Analytical Instrumentation, Madison, WI, **1996**.

Received: March 9, 2006